

# We are IntechOpen, the world's leading publisher of Open Access books Built by scientists, for scientists

6,900

Open access books available

185,000

International authors and editors

200M

Downloads

Our authors are among the

154

Countries delivered to

TOP 1%

most cited scientists

12.2%

Contributors from top 500 universities



WEB OF SCIENCE™

Selection of our books indexed in the Book Citation Index  
in Web of Science™ Core Collection (BKCI)

Interested in publishing with us?  
Contact [book.department@intechopen.com](mailto:book.department@intechopen.com)

Numbers displayed above are based on latest data collected.  
For more information visit [www.intechopen.com](http://www.intechopen.com)



# Crystalline Silicon Nitride Films on Si(111): Growth Mechanism, Surface Structure and Chemistry down to Atomic Scale

*Subhashis Gangopadhyay*

## Abstract

A detailed investigation of the growth mechanism of ultra-thin silicon nitride ( $\text{Si}_3\text{N}_4$ ) films on Si(111) substrates, their structure, morphology and surface chemistry down to atomic scale have been investigated using various surface analytical techniques such as low energy electron diffraction (LEED), scanning tunneling microscopy (STM) and ESCA microscopy. A radio frequency  $\text{N}_2$  plasma source from Epi Uni-bulb has been used for the nitridation of atomically clean Si(111) surfaces. The substrate temperatures during the nitridation process were ranging from 600–1050°C and the plasma exposure times were varied from 5 s for initial nucleation up to 45 min for saturation thickness. The initial stage of N nucleation on Si(111), how the structure and morphology of the nitride films depend on thickness and temperature, surface atomic reconstructions and the nitride film chemical composition are discussed here. All findings are explained in terms of thermally activated inter-diffusion of Si and N atoms as well as the surface adatom diffusion/mobility.

**Keywords:** silicon nitride thin film, growth mechanism, surface reconstruction, STM, LEED

## 1. Introduction

In semiconductor technology, one of the most important parts is the formation of homogeneous insulating layers and are of high practical importance as it is an integral part all kinds of integrated circuits. Due to the recent miniaturization in nanotechnology, insulating layer thickness needs to be precisely controlled down to a few nanometer ranges. This nanometer scale insulating films not only reduce the devices size, but also provide a platform for novel device fabrication such as resonant tunneling diodes [1] or memory devices for magnetic tunnel junction [2].

Since last few decades,  $\text{SiO}_2$  on silicon (Si) is found to be the most useful insulating material in VLSI device technology because of its high quality and superior homogeneity. However, continuous miniaturization of device size now demands a thickness of this insulating layer down to a few atomic layers. Here, the homogeneity of the insulating film in terms of morphology and chemical purity becomes more pronounced. Very small fluctuations in thickness of the oxide layer may lead

to the break-down due to the enhanced electron tunneling as this insulating barriers is extremely thin. Hence, demand for new materials with a higher dielectric constant is of high priority which can replace the  $\text{SiO}_2$  layer to overcome this issue. In this regard, crystalline silicon nitride ( $\text{Si}_3\text{N}_4$ ) films received considerable attention to replace the existing  $\text{SiO}_2$  gate dielectric materials, as it is compatible with existing Si processing technologies as well as larger dielectric constant and diffusion resistive materials properties [3, 4]. Plasma assisted amorphous silicon nitride layer has recently been used as high performance gate dielectric [5]. High thermal stability and refractive index of  $\text{Si}_3\text{N}_4$  make it capable for high temperature structural ceramics and anti-reflective coating materials, respectively. Finally, crystalline  $\text{Si}_3\text{N}_4$  on Si can also serve as a substrate for highly demanding GaN growth to integrate the opto-electronic devices to the well-established silicon based device technology [6, 7]. Therefore, better understanding of the initial  $\text{Si}_3\text{N}_4$  films growth on Si, their structural and morphological evolution as well as chemical properties in a very local (atomic) scale are of high technological importance.

### 1.1 Structure and properties

Silicon nitride is a structural ceramics, which exhibits high mechanical strength at room as well as elevated temperature. It can also be useful because of its high fracture toughness. It shows a very high thermal stability, up to  $1600^\circ\text{C}$  in air and also has a much larger dielectric constant ( $\epsilon = 7.5$ ) as compared to the conventional  $\text{SiO}_2$  ( $\epsilon = 3.8$ ). It is a semiconducting material with an energy band gap of about 4.7 eV, which is almost half of  $\text{SiO}_2$  (9 eV). Usually the bulk  $\text{Si}_3\text{N}_4$  has been produced by sintering method and structurally appeared as poly-crystalline ceramic. Crystalline silicon nitride appears with two different phases, such as  $\alpha$ -phase and  $\beta$ -phase of  $\text{Si}_3\text{N}_4$ . Both the phases have space groups of  $P31_c$  and  $P6_3$  for  $\alpha$ - and  $\beta$ - $\text{Si}_3\text{N}_4$ , respectively and the structures appeared with a hexagonal symmetry. Although there were some contradiction about these two phases, finally it has been well accepted that the only stable phase is the  $\beta$ - $\text{Si}_3\text{N}_4$  phase whereas the  $\alpha$ - $\text{Si}_3\text{N}_4$  phase is a meta-stable one and has a lattice constant along c-axis (0001) just double of the  $\beta$ -phase.

Various groups have already described the crystal structure of  $\beta$ - $\text{Si}_3\text{N}_4$  and for the bulk crystals. A lattice constant of ' $a$ ' = 7.595 Å in the hexagonal (X-Y) plane whereas ' $c$ ' = 2.902 Å in the vertical (Z) direction are obtained [9]. A schematic model of the  $\beta$ - $\text{Si}_3\text{N}_4$  structure (top view), containing 14 atoms in the lateral plane (normal to c-axis) can be seen in **Figure 1** where half of the atoms are placed below (at  $Z = -c/4$  plane) and the other half above (at  $Z = c/4$  plane) the X-Y plane. Local geometrical configuration indicates a combination of  $sp^3$  and  $sp^2$  hybridized orbital for Si and N atoms, respectively. This structure can also be considered as tetrahedrons of  $\text{Si}_3\text{N}_4$  complex network, connected through their corners. Further structural information of  $\beta$ -phase of silicon nitride and how it is related to the  $\alpha$ -phase has also be reported elsewhere [8, 9].

### 1.2 Different approaches

Formation of crystalline silicon nitride films has been performed using various growth methods. Chemical vapor deposition (CVD) growth process has been used to grow silicon nitride where a mixture of silicon-hydrogen ( $\text{SiH}_4$ ,  $\text{Si}_2\text{H}_6$ ,  $\text{Si}_3\text{H}_8$ ) and nitro-hydro compounds ( $\text{NH}_3$ ,  $\text{N}_2\text{H}_4$ ,  $\text{HN}_3$ ) are used. In general, resulting films are usually appeared in an amorphous phase, non-stoichiometric and significantly contaminated [10]. However, without supplying any Si - $\text{H}_2$  source compound, it also possible to obtain nitride layers by direct nitridation of a Si substrate at elevated

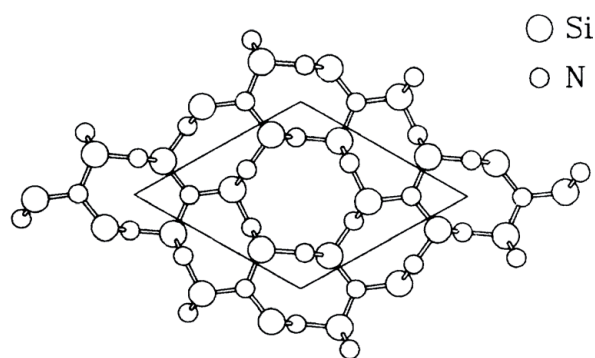


**Figure 1.** Schematic top (0001) view of the  $\beta$ - $\text{Si}_3\text{N}_4$  structure model in a lateral ( $x$ - $y$ ) plane with 14 atoms. The bigger and smaller circles represent the Si and N atoms respectively, whereas the parallelogram indicates the unit cell [8].

temperature. Si(111) surface exhibits a threefold rotational symmetry. Moreover, its  $2 \times 2$  unit cell is having a lattice mismatch of only about 1.1% with the 'a' axis of hexagonal  $\text{Si}_3\text{N}_4$ . These two properties make it a very compatible substrate for the growth of  $\text{Si}_3\text{N}_4$  films in the (0001) lattice direction. It can be done by exposing the atomically clean Si substrate to various  $\text{N}_2$  compound reactive gases such as  $\text{NH}_3$  [11–17],  $\text{NO}$  [18–21] or other gaseous at high nitridation temperatures or by post exposure thermal annealing. In addition, ion bombardment methods [22–25] or sputter deposition technique have also been employed. However, use the pure nitrogen gas would be the simplest and easiest way for the nitridation of the Si surface. But a very high growth pressure is required due to the inertness of molecular nitrogen. This may lead to a huge out gassing and finally lead to a severe contamination within the nitride film. If we can provide an atomic nitrogen source, this problem can be solved. Therefore, nitrogen plasma sources can be used for the exposure of active nitrogen flux on Si surface. The atomic nitrogen exposure on Si(111) and Si(001) surfaces at relatively lower nitridation temperatures leads to the formation of amorphous nitride layer and appears with a highly disorder interface of nitride/Si. However, a crystalline interface and well-ordered films of hexagonal  $\beta$ - $\text{Si}_3\text{N}_4$  films have only been observed for nitridation temperature only above  $700^\circ\text{C}$  [13–17, 22–27]. Epitaxial  $\beta$ - $\text{Si}_3\text{N}_4$  formation on Si(111) by thermal annealing of N-irradiated Si(111) surface has been reported by Yamabe et al. [28]. Silicon nitride growth kinetics and surface thermodynamics at elevated temperature under ammonia exposure is recently been reported [29].  $\text{N}_2$ -plasma assisted surface nitridation of Si(111) followed by vacuum annealing at high temperature ( $900^\circ\text{C}$ ) results in a better quality  $\text{Si}_3\text{N}_4$  film [30].

Various analytical characterization methods have been employed to investigate the growth mechanism and structural properties of thermally grown nitride layers. In general, surface probing instruments collect the information on lateral averaging over the surface. As diffraction method, low energy electron diffraction (LEED), reflected high energy electron diffraction (RHEED) [28–29] are used for surface whereas low angle X-ray diffraction (XRD) is used for interface studies. Similarly, to investigate the chemical properties as well as bonding configuration, Auger electron spectroscopy (AES), photoelectron spectroscopy with X-ray (XPS) and ultraviolet light (UPS), electron energy loss spectroscopy (EELS), thermal desorption spectroscopy (TDS) etc. have been used. However, for atomic scale local information such as growth kinetics and surface reconstructions, direct microscopic imaging using low energy electron microscopy (LEEM), atomic force microscopy and scanning tunneling microscopy have been utilized. X-ray reflectivity (XRR) has also been carried out in some cases, to find the information about nitride layer thickness and subsurface interface.



## 2. Experimental details

Highly oriented p-type Si(111) wafers (boron doped, 0.02° miscut angle) were used as substrates and a clean Si(111) surface with well reconstructed  $7 \times 7$  structure was prepared prior to the nitridation process. This preparation was routinely checked by both LEED and STM, and a clear  $7 \times 7$  reconstruction was reproducibly observed. The sample temperature was measured using an infrared pyrometer with an uncertainty of 20°C. Si substrate nitridation process was performed by exposing the  $7 \times 7$  reconstructed clean Si(111) surface to atomic nitrogen flux at different substrate temperatures. A commercial radio frequency (RF) plasma source from Epi Uni-bulb was used as atomic nitrogen sources. Plasma chamber pressure was maintained at about  $10^{-5}$  mbar during plasma discharge. The pressure was controlled by a leak valve connected to the inlet line of  $N_2$  gas. The plasma source was operated at with a RF power of 450 W. The exposure time of the active nitrogen flux on Si substrate was varied such a way that the coverage of the nitride films starts from sub-monolayer and ends up to the saturation thickness. Crystalline quality and surface reconstructions of the nitride layer were characterized by LEED. The surface morphology, growth kinetics, as well as nucleation process and the real space atomic structure were studied using an in-situ STM. Chemical composition and stoichiometry of the film are studied using ESCA microscopy and X-ray photoelectron spectroscopy, which finally provides the information about film thickness and its homogeneity.

## 3. Results

### 3.1 LEED results

An average information about the  $Si_3N_4$  surface reconstruction grown on Si(111) and its crystalline quality after the nitridation process at different substrate temperatures ranging from 600–1100°C, have been investigated using low energy electron diffraction (LEED) method. Prior to any nitride formation, clean Si(111) surface appears with a sharp  $7 \times 7$  LEED patterns. LEED patterns appear with a very faint “ $8 \times 8$ ” reconstruction for nitridation below 600°C. This finding indicates a poor crystallinity of the nitride films and mostly amorphous silicon nitrides later is formed. With increasing nitridation temperature, crystalline quality of the nitride films drastically improves and appears with a sharp “ $8 \times 8$ ” LEED patterns. After nitridation for about 15 min under the RF-plasma source at different temperatures, the evolution of the “ $8 \times 8$ ” structures has been shown in **Figure 2**. The LEED patterns of clean Si(111)- $7 \times 7$  have been shown in **Figure 2(a)**. The yellow and cyan circles represent the (0,0) and (1,0) diffraction spots of the reconstructed Si(111) surface. After nitridation at 700°C, faint diffraction spots of  $Si_3N_4$ -“ $8 \times 8$ ” structure (1, 0) starts to appear. Increase the nitridation temperature results in a much brighter LEED spots along with an additional faint superstructures of “ $8/3 \times 8/3$ ” [6]. In case of a further increase in nitridation temperature to 920°C (**Figure 2(b)**), the LEED patterns get significantly sharpen. The “ $8/3 \times 8/3$ ” superstructures (red circles) appear in a much brighter contrast and dominate in lower beam energy. From the positions of the diffraction spots of the  $Si_3N_4$ -“ $8 \times 8$ ” structure and comparing those with the initial Si(111) diffraction spots, a periodicity of about 2.79 Å has been observed for the “ $8 \times 8$ ” structures. However for the “ $8/3 \times 8/3$ ” superstructures, the periodicity appears to be 10.2 Å.

For surface nitridation above 950°C, another type of surface reconstruction of  $Si_3N_4$ /Si(111) appears in LEED pattern, which is known as the ‘quadruplet structure’ or  $3/4 \times 3/4$  reconstruction. This pattern appears in coexistence with

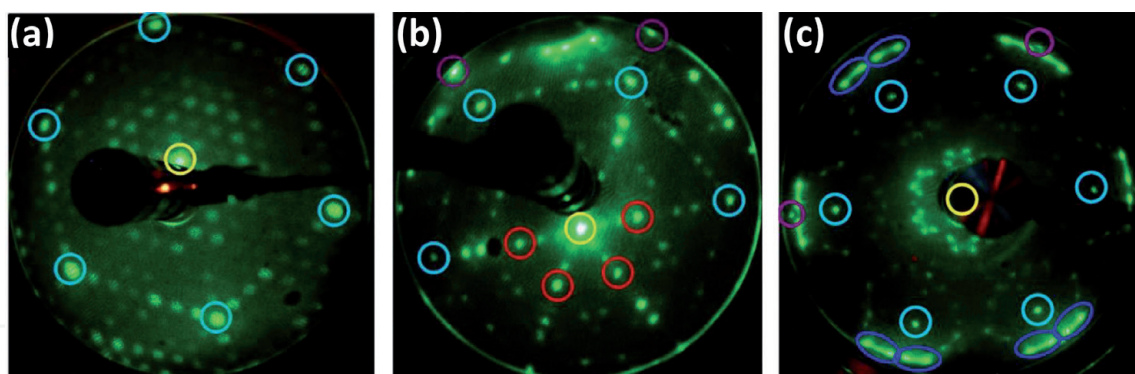


**Figure 2.** LEED patterns show the evolution of the  $\text{Si}_3\text{N}_4$ -“structure with increasing nitridation temperature”. (a) Clean  $\text{Si}(111)$ - $7 \times 7$  structure: Yellow and cyan circles correspond to the (0,0) and the (1,0) diffraction spots. (b)  $\text{Si}_3\text{N}_4$ -“ $8 \times 8$ ” structures: Purple circles corresponds to the (1,0) diffraction spots of  $\text{Si}_3\text{N}_4$ -“ $8 \times 8$ ” structures, whereas the “ $8/3 \times 8/3$ ” superstructures are indicated by red circles (nitridation at  $920^\circ\text{C}$ , electron beam energy 43 eV). (c)  $\text{Si}_3\text{N}_4$  ‘quadruplet structures’: Intense quadruplet structures are indicated by blue ellipses, whereas the (1,0) diffraction spots of the  $\text{Si}_3\text{N}_4$ -“ $8 \times 8$ ” structure are represented by the purple circles (nitridation at  $1050^\circ\text{C}$ , electron beam energy 52 eV).

the existing “ $8 \times 8$ ” structure. With further increasing in nitridation temperature, the quadruplet structure starts to dominate over the “ $8 \times 8$ ” patterns. Clear LEED patterns of quadruplet structure have been observed only above  $1000^\circ\text{C}$  (**Figure 2(c)**). This is appeared in bright spots (blue ellipse) with the crystalline domains angular rotations of  $\pm 5^\circ$  and  $\pm 10^\circ$ , with respect to the underlying Si lattice. The (1, 0) spots of the  $\text{Si}_3\text{N}_4$  “ $8 \times 8$ ” structure has also been observed within the purple circles. By comparing the quadruplet structure LEED spots with the (1, 0) diffraction spot of  $\text{Si}(111)$ , a surface lattice periodicity of about  $2.88 \text{ \AA}$ , has been observed for the quadruplet structures. It has been observed that the quadruplet structures usually appear with a contaminated surface, sometimes even at lower nitridation temperatures [13, 31].

### 3.2 STM results

Exposure of atomic nitrogen on the  $\text{Si}(111)$  surface at elevated substrate temperatures results in silicon nitride formation. A clear understanding of the silicon nitride growth mechanism and its impact on the structural properties of the as grown film is of high fundamental interest. STM studies of various silicon nitride films after nitridation at various temperatures, as well as  $\text{Si}_3\text{N}_4$  film thicknesses starting from sub-monolayer coverage up to the saturation thickness can be seen here. The initial nucleation stage of silicon nitride films, their various growth steps along with the evolution of surface morphology and finally surface atomic structures of are discussed with atomic precision.

**Initial nucleation:** In order to understand how the initial nucleation mechanism takes place and the absorption of N atoms on Si surface to form nitride layer, sub-monolayer coverage of  $\text{Si}_3\text{N}_4$ -“ $8 \times 8$ ” structures formation on  $\text{Si}(111)$  surface have been studied here. After a plasma exposure for 5 s, many small nucleation pits starts to appear within the terraces of the  $\text{Si}(111)$  surface (dark spots) as well as step edges exhibit many discrete nucleation patches within the upper terrace (also appeared in darker contrast) (**Figure 3**). For simplicity, henceforth, we will be mention those dot-like dark structures within the terrace area as ‘nucleation pits’ and refer those step edge patches as the ‘nucleation patches’ [32]. With increase in nitridation temperature, it has been observed that the density of the nucleation pits/patches both within terraces or at the step edges are significantly decreased, whereas the average size has drastically increased (**Figure 3**). Usually, the nucleation patches are larger in size as compared to



the nucleation pits. Moreover, larger etch pits preferentially appear along the initial Si(111)- $7 \times 7$  domain boundaries. For nitridation above 800°C, shape of the dark nucleation pits becomes regular (equilateral triangle). Triangular nucleation patches at the upper terrace of the step edges are also observed where the apex of the triangles point towards the  $[-1 -1 2]$  crystal direction, away from the steps. This direction of the nitride pit/patch growth is determined by comparing the faulted and unfaulted half unit cell of the Si(111)- $7 \times 7$  (**Figure 3(d)**). A closer view STM image of this nitrified surface is shown in **Figure 4** (nitridation at 800°C). Nucleation etch pits of triangular

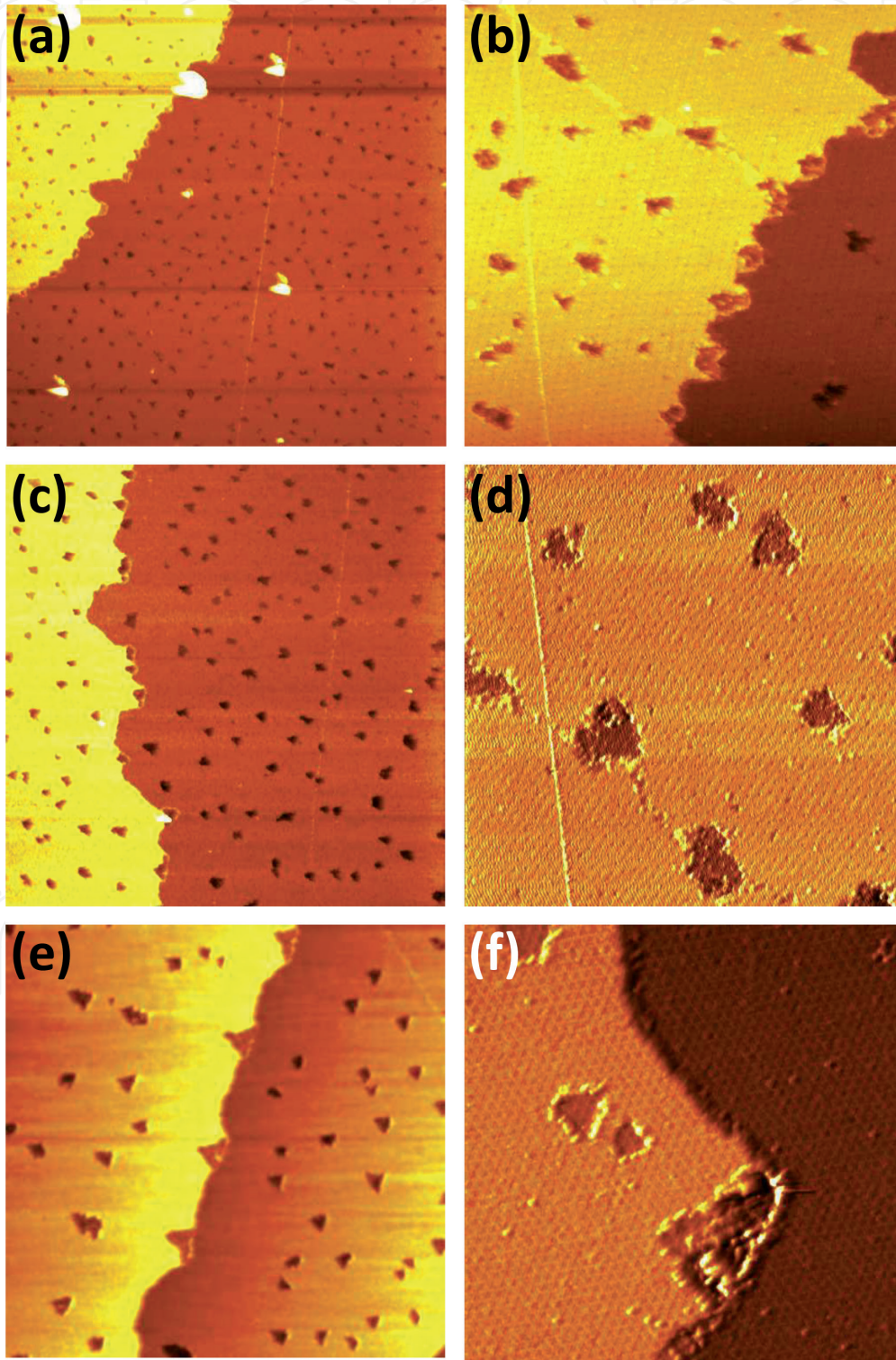


**Figure 3.** STM images of submonolayer coverage silicon nitride nucleation with nitridation temperatures: [(a) and (b) 720°C, (c) and (d) 760°C, and (e) and (f)] 800°C, respectively, using rf-plasma exposure for 5 s. Scan areas: (a), (c) and (e)  $400 \times 400 \text{ nm}^2$  and (b), (d) and (f)  $100 \times 100 \text{ nm}^2$ .

pattern can clearly be seen. Surprisingly, both nucleation pits appear with a clean Si(111)- $7 \times 7$  structure with 1.5 Å lower than the Si terrace. Si and/or N adatoms are preferentially found around the outer periphery of the  $7 \times 7$  nucleation pits and in STM image appear as bright dots (**Figure 4**). Sometimes, adatoms have also found within the larger nucleation pits. However, nucleation patches located at the step edges generally shows a disordered structure in STM imaging. **Figure 4** shows an interesting feature where a transition from Si(111)- $7 \times 7$  nucleation patches to initial nucleation of “ $8 \times 8$ ” structures at the step edge has been observed. Inner side of the step shows an atomically resolved Si(111)- $7 \times 7$  structure, whereas outer side of the step shows a Si<sub>3</sub>N<sub>4</sub>-“ $8 \times 8$ ” structure. Comparing the height difference it is confirmed that the patch appears with a similar height scale as the pits within terrace (1.5 Å, lower/higher) than the (upper/lower terrace). Furthermore, the Si(111)- $7 \times 7$  structure exhibits the same rotational symmetry within nucleation pits and nucleation patches, having only translational shifts. Nitridation at 850°C results in atomically resolved honey-comb structures (“ $8 \times 8$ ”) of Si<sub>3</sub>N<sub>4</sub>. In this case, Si(111)- $7 \times 7$  structures are not found any more within the nucleation site.

**Effect of annealing:** The effect of the post-exposure thermal annealing at different temperatures for sub-monolayer coverage nitride films grown at 800°C is shown here in **Figure 5**. STM images depict the evolution of Si(111) surface after 800°C nitridation for 30 s, using RF-plasma source followed by subsequent post-annealing for one minute at 850°C and 900°C, respectively. As expected, nucleation pits (Si(111) terrace area) and nucleation patches (upper terrace of step edge) of triangular shapes are formed after 30 s nitridation at 800°C (**Figure 5(a)** and **(b)**), with an enhanced density and size as compared to earlier result presented in **Figure 4(e)** (5 s nitridation). After annealing at 850°C for 1 min, thermal energy increases the surface adatoms mobility, which significantly changes the surface morphology as shown in (**Figure 5(c)** and **(d)**). It has been observed that those triangular pits located away from the surface steps are not affected much, however, the patches/pits at the surface steps/close proximity of lower steps, are strongly affected. Some of the patches form free standing islands of silicon nitride getting detached from the upper terrace. Moreover, free standing nitride islands also appear in larger size, due to the coalescence between nucleation patches and pits. Comparing with earlier images (**Figure 5(a)**), it can be concluded that the surface steps are locally retracted towards the upper terrace, leading towards the formation of free standing nitride islands within the lower terrace

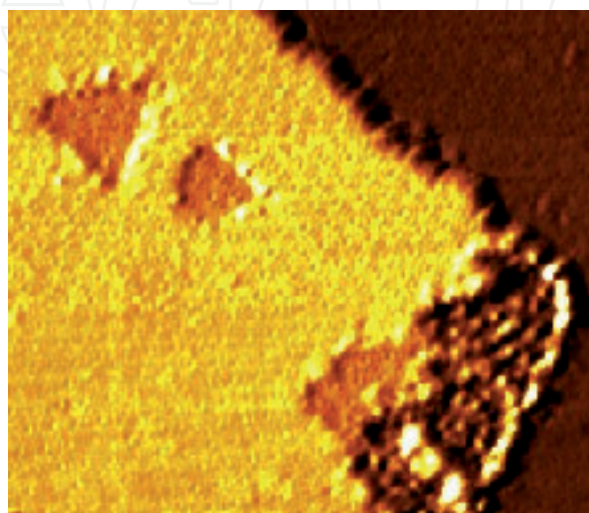


**Figure 4.**  
Closer view STM image shows the formation of nucleation pits within Si(111)- $7 \times 7$  surface terrace and at the step edge (nitridation at 800°C for 5 s). Scan areas  $65 \times 60 \text{ nm}^2$ .



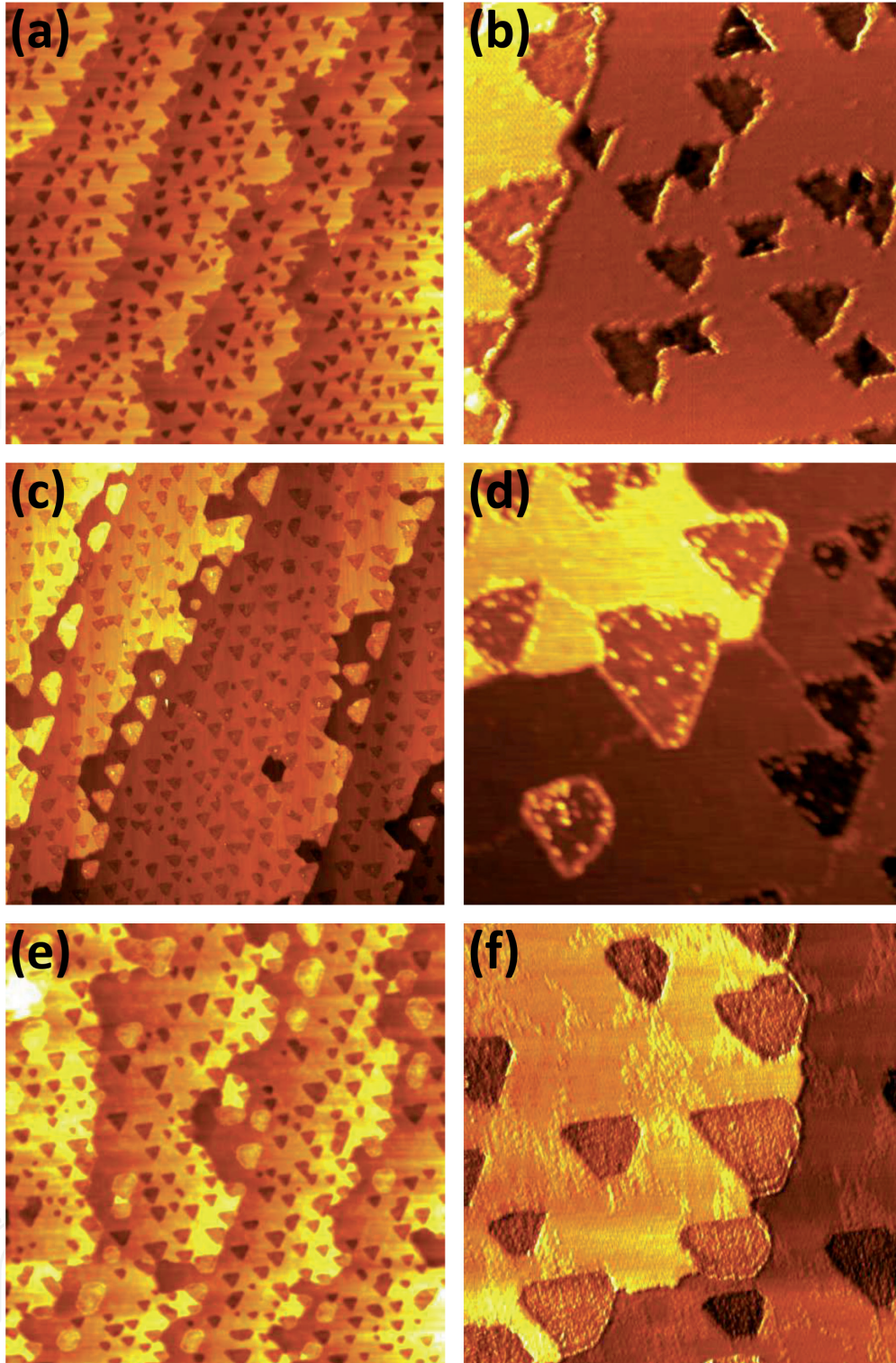


**Figure 5.** STM images of evolution of Si(111) surfaces: (a) and (b) after nitridation at 800°C for 30 s, (c) and (d) post annealing at 850°C for 60 s, and (e) and (f) further post annealing at 900°C for 60 s, respectively. Scan areas: (a), (c) and (e)  $1 \times 1 \mu\text{m}^2$  and (b), (d) and (f)  $200 \times 200 \text{ nm}^2$ .

area. The shape of the free standing nitride islands also differs from the triangular pits/patches which have been discussed in later. Resulting changes in nitride surface morphology, after annealing at 900°C for another minute can be seen in **Figure 5(e)** and **(f)**. Further movement of the surface steps towards upper terrace and enlargement of the free standing nitride islands have been observed. Eventually, this effect may lead to a terrace breaking. In addition, nucleation of N adatoms at the initial  $(7 \times 7)$  domain boundary regions has also been taken place, (appears as bright dots within the terrace), leading to the inter connection between two nitride pits/islands (**Figure 5(f)**).

The closer view STM images of free standing nitride island and nitridation at the initial domain boundary of Si(111)- $7 \times 7$  surface are shown in **Figure 6**. The  $\text{Si}_3\text{N}_4$  structures are now appeared with an ordered atomic arrangement of a honeycomb-like " $8 \times 8$ " (**Figure 6**). Within islands/pits, Si(111)- $7 \times 7$  structures are not observed any more. A clearer appearance of the " $8 \times 8$ " structure also suggests a drastic improvement in nitride films crystalline quality. Apart from the structural improvements, the shape and size of nitride nucleation centers have significantly been altered. The " $8 \times 8$ " nucleation pits within the terrace area remain still triangular, however, the free standing islands become in truncated shape and start to become a hexagonal shape as shown in **Figure 6(a)** [32]. Direct nucleation of nitride layer (without forming pit/patch) has also started after second step of annealing at  $900^\circ\text{C}$ , at the domain boundary regions of initial the  $7 \times 7$  terrace, as can be seen as bright dots in **Figure 6(b)**. This way, nitride layer connects between two different nucleation pits/islands and further proceeds to form a continuous layer on Si surface. The structural quality of the " $8 \times 8$ "- $\text{Si}_3\text{N}_4$  layer has also been improved with the nitridation/annealing temperature, which is also in agreement with our earlier LEED observations.

**Thickness dependent surface morphology:** STM images show the morphological evolutions of crystalline silicon nitride films grown on Si(111) surface at  $850^\circ\text{C}$  have been compared here with an increasing exposure durations of RF nitrogen-plasma. Structure and morphological evolution of Si(111) surface, exposed for nitridation for (a) 2 min, (b) 4 min, (c) 12 min and (d) 45 min, respectively, using RF-plasma are presented in **Figure 7**. Initial Si surface gets completely covered by " $8 \times 8$ " nitride layer after an exposure of RF plasma for 2 min (**Figure 7(a)**). Large  $\text{Si}_3\text{N}_4$  islands with atomically flat top surfaces are observed throughout the surface. Initial terrace structure of Si(111)- $7 \times 7$  substrate gets completely broken and some of the nitride islands appear significantly higher (few bilayer steps of Si(111)) due to the effect of step bunching. Atomically resolved honeycomb-like structures of  $\text{Si}_3\text{N}_4$  with " $8 \times 8$ " periodicity are obtained throughout the surface as shown within the inset of **Figure 7(a)**. For even longer exposure of RF-plasma, a thicker nitride layers is formed. The surface morphology of the nitride film grown after 4 min of nitridation is shown in **Figure 7(b)**. The surface appears in rough morphology with many grooves and holes and the initial terrace structures of Si(111) get partially broken. For even longer nitridation of 12 min a very different surface morphology is observed. Si(111) terrace structures are completely broken and large 2D islands with a flat top surfaces formed (**Figure 7(c)**). Step heights of these nitride islands

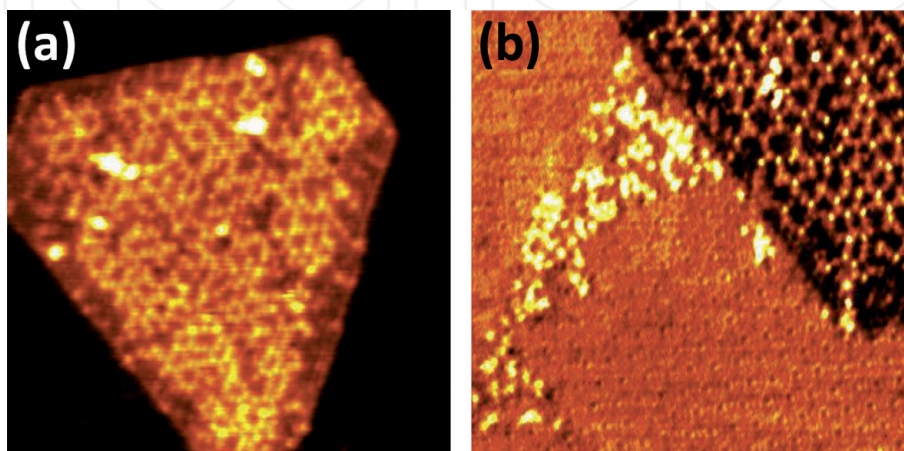


**Figure 6.**  
 Closer view STM images of (a) free standing nitride island detached from the step edge and (b) nitride formation within etch pit in the terrace area and in domain boundary.



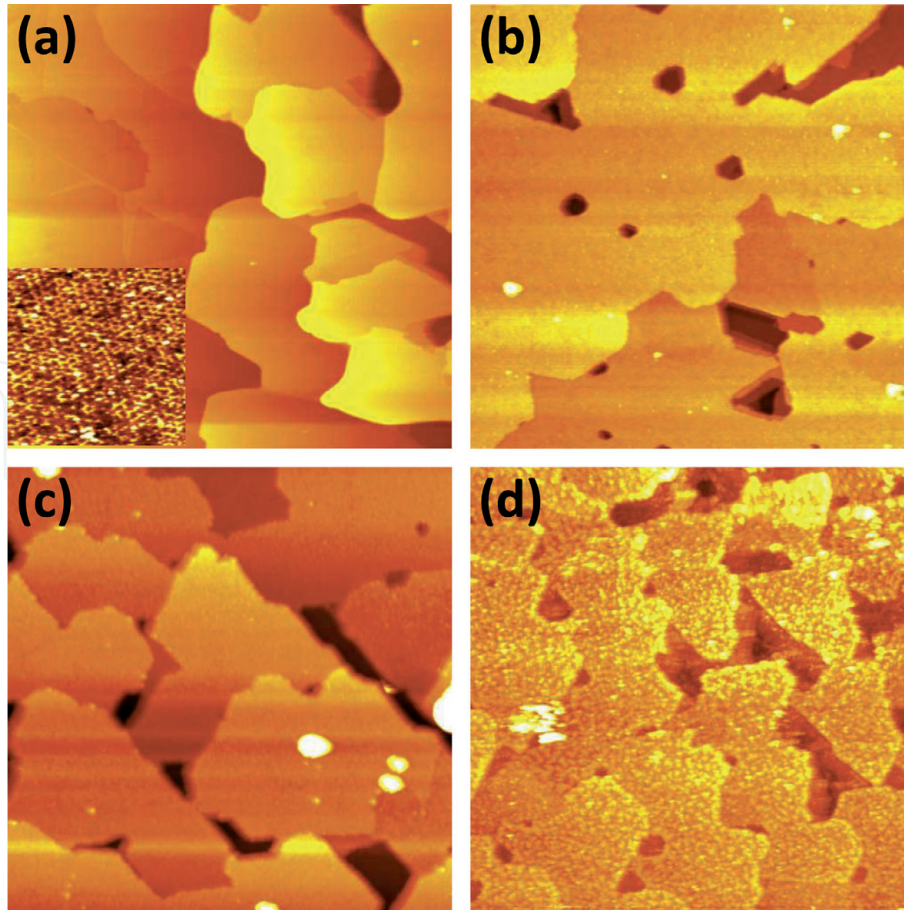


**Figure 7.** STM images of silicon nitride film grown at 850°C with increasing duration of RF-plasma: (a) 2 min, (b) 4 min, (c) 12 min and (d) 45 min, respectively. Scan area:  $1 \times 1 \mu\text{m}^2$ . Inset of (a) shows atomically resolved honey comb structure of “8 × 8”-  $\text{Si}_3\text{N}_4$ .

are found to be an integer multiple of 2.9 Å. This finding suggests the formation of multilayer  $\beta\text{-Si}_3\text{N}_4$ . It also indicates the crystalline correlation of the as grown nitride film with the Si(111) substrate, such as:  $\text{Si}_3\text{N}_4$  (0001)  $\parallel$  Si(111). Moreover, the holes and grooves appear even larger and deeper. In addition, the border of the nitride islands appears in a straight line manner. Very similar kind of structure is also observed within the holes and grooves. This observation confirms the formation of nitride layer within the holes/grooves and as a result finally a continuous  $\text{Si}_3\text{N}_4$  layer is formed. After 45 min of nitridation, the  $\text{Si}_3\text{N}_4$  film reaches to its saturation thickness as the surface morphology changes drastically (**Figure 7(d)**). Overall surface roughness is somewhat decreased. Holes/grooves are partially filled as they become smaller in size as well as shallower in depth. Along with, the top nitride surface becomes very granular and appears with many small clusters/blobs. A very similar kind of finding has also been reported in STM studies [29].

**Surface reconstructions of  $\beta\text{-Si}_3\text{N}_4$ :** Depending upon the nitridation parameters (temperature and duration), generally two types of silicon nitride surface reconstructions are observed in STM: (a) honeycomb-like “8 × 8” structures with a surface periodicity of 30.7 Å and (b) “8/3 × 8/3” superstructures of 10.2 Å surface periodicity. High temperature nitridation (> 1000°C) usually results in a so called ‘quadruplet structures’ (3/4 × 3/4) in LEED observation, however, atomically resolved structures of 3/4 × 3/4 reconstructions are not found in our STM study.

**Honeycomb-like “8 × 8” reconstruction:** A honeycomb-like “8 × 8” surface reconstruction of silicon nitride films are only observed in STM for a very thin  $\text{Si}_3\text{N}_4$  films, having coverages below 2 ML. These honeycomb-like structures usually start to appear at relatively lower nitridation temperature (800°C) with high defect



density with a poor order of crystal symmetry. Increase in nitridation temperature or post-nitridation thermal annealing (higher temperatures) significantly improves the ordering and structural symmetry. However, a thicker nitride film does not show any well resolved honeycomb-like surface in STM imaging.

Empty state STM images of  $\text{Si}_3\text{N}_4$  surface grown at  $850^\circ\text{C}$  are shown in **Figure 8(a)** and **(b)**. Honeycomb-like “ $8 \times 8$ ” surface reconstruction of  $\text{Si}_3\text{N}_4$  surface is formed after 30 s of RF-plasma nitridation. The structure appears as a defective and in quasi-periodic network of local disordering (**Figure 8(a)**). A closer view of this honeycomb-like structures nicely resolved with atomic resolution is depicted in **Figure 8(b)**. However, the short range lattice disorders can also be observed here along with the loop like structures. These disordered state can be attributed to the interfacial states of  $\text{Si}_3\text{N}_4/\text{Si}(111)$ . An autocorrelation of this surface shows a periodicity of about  $30.6 \text{ \AA}$ , indicating a “ $8 \times 8$ ”-  $\text{Si}_3\text{N}_4$  structure [32].

**“ $8/3 \times 8/3$ ” surface reconstruction:** Apart from this “ $8 \times 8$ ” surface reconstructions, in case of relatively thicker  $\text{Si}_3\text{N}_4$  films grown at a temperature between  $900$  and  $980^\circ\text{C}$ , another type of surface reconstructions known as “ $8/3 \times 8/3$ ” superstructure is also observed. A surface periodicity of  $10.2 \text{ \AA}$  is found here and the empty state STM images of well reconstructed “ $8/3 \times 8/3$ ” structures appears with a long range symmetry, as shown in **Figure 8(c)** and **(d)**. The nitride film was formed by 20 min of RF-plasma exposure on clean  $\text{Si}(111)$  surface at  $950^\circ\text{C}$ . A long range atomic symmetry of “ $8/3 \times 8/3$ ” structure is nicely resolved here. This result also suggests that a highly crystalline  $\text{Si}_3\text{N}_4$  films can also be formed by a systematically choosing the nitride growth parameters. However, few defect areas on this surface such as vacancies/missing atoms (dark areas) as well as adatoms (bright

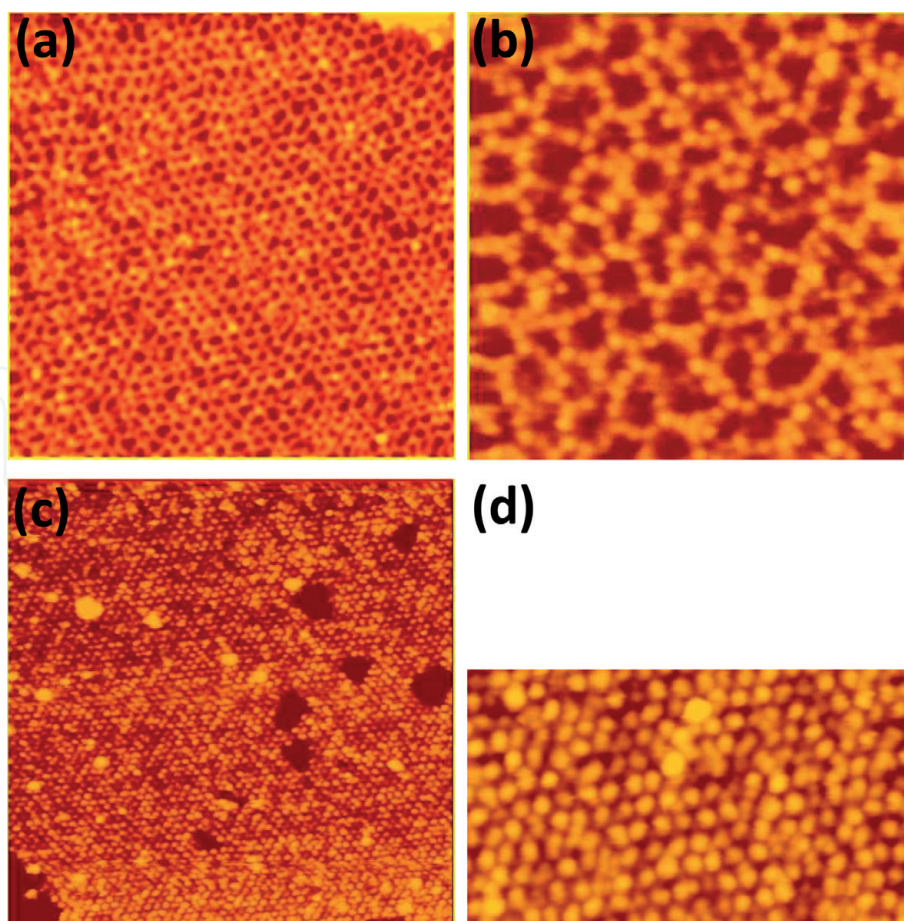


**Figure 8.**  
 Empty state STM images of  $\text{Si}_3\text{N}_4$  surface showing atomically resolved surface of: (a) and (b) honey-comb like “ $8 \times 8$ ” surface reconstructions (3 V) and (c) and (d)  $8/3 \times 8/3$  surface reconstructions (4 V).

areas) have also been observed. A closer view of this “ $8/3 \times 8/3$ ” surface can be seen in **Figure 8(d)**. Here, a weak modulation with 3-fold surface symmetry can also be observed by a careful inspection. This effect might be related to the coexistence of the “ $8 \times 8$ ” LEED spots along with the “ $8/3 \times 8/3$ ” superstructure spots of nitride films. An autocorrelation measurement of this superstructure is also performed which shows a structural periodicity of about 10.2 Å, confirming the formation of “ $8/3 \times 8/3$ ” superstructure [6, 30].

### 3.3 ESCA results

Apart from STM imaging, ESCA microscopy technique is also employed to investigate the surface chemical properties of the thin silicon nitride films grown on clean Si(111) substrates. Contrast observed in ESCA microscopy image usually occurs from two factors: (a) chemical inhomogeneity, i.e., any kind of compositional fluctuation and (b) film thickness inhomogeneity, i.e., surface roughening leading towards nitride layer thickness fluctuation. To perform a comparative study, two types of nitride samples are used here. In one hand, a flat and smooth nitride film grown at a relatively low nitridation temperature is used. In other hand, nitride film with a rough surface morphology grown by nitridation at higher temperature is tested.

In case of smooth nitride films, a very weak modulation in ESCA image contrast has been observed for both scans using Si-2p bulk and nitride binding energies (images not shown here). ESCA microscopy image using N-1 s components also appears in a very similar manner. Both findings indicate towards the surface chemical homogeneity of the nitride film. To further confirm the chemical uniformity of this surface, high resolution XPS study has also been tested using of Si-2p photoemission line. A chemical shift of 2.9 eV has been found within the Si-2p spectra. This information can suggest the nitride film stoichiometry and in good agreement with the reported literature for  $\text{Si}_3\text{N}_4$  compound formation [33, 34]. The thickness of the nitride film can also be estimated using this known  $\text{Si}_3\text{N}_4$  stoichiometry. Total integral intensities of both nitride and bulk Si-2p components are used to calculate the film thickness. A detailed analysis of the nitride film thickness calculation has already been reported elsewhere [35, 36].

However, for nitride films of rough surface morphology, grown at higher nitridation temperatures appear with a strong contrast in ESCA microscopy images as shown in **Figure 9**. Photoelectron signals from: (a) N-1 s line and (b) Si-2p bulk line are used for the spectro-micrographs here. An inverted contrast in ESCA microscopy images is observed here appear with a strong contrast (**Figure 9(a)** and **(b)**). This finding can be explained in terms of nitride film thickness fluctuation. The existence of any bare Si(111) surface can be excluded from our earlier STM observations, where a continuous nitride layer with a thickness modulation was observed for this type of nitridation process.

In case of a smooth and uniform nitride films, the contrast in ESCA microscopy image for N-1 s line can be attributed to silicon nitride film stoichiometry, i.e., chemical inhomogeneity. In that case, Si-2p bulk component should be homogeneous and the ESCA microscopy is expected to be without any significant imaging contrast. In contrast, however, a strong contrast is observed also for the Si-2p bulk line. It is a clear indication of thickness fluctuation rather any chemical inhomogeneity within the nitride film. **Figure 9(c)** and **(d)** show a further investigation related to the film thickness variation of nitride films. **Figure 9(c)** shows a closer view of ESCA micrograph using the N-1 s line. Individual XPS spectra of the Si-2p binding energy measured at two different locations (marked bright and the dark areas within the ESCA micrographs) are recorded and the correlation between these



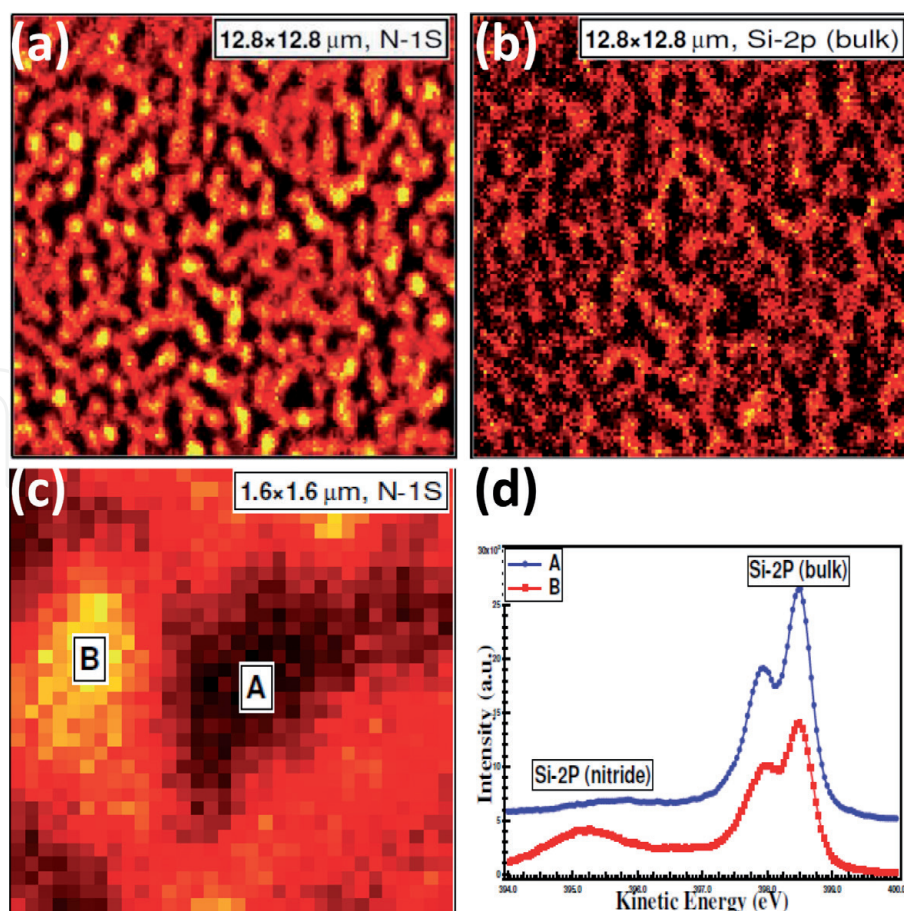


**Figure 9.** ESCA micro-spectrograph of silicon nitride film grown at relatively higher nitridation temperature (950°C) (a) with N-1 s line, (b) with Si-2p bulk line, (c) closer view with N-1 s line and (d) Si-2p XPS spectra at the corresponding location mentioned within image (c).

two spectra is compared (**Figure 9(c)**). Both spectra clearly indicate the contrast within the ESCA micrograph is mostly due to the lateral fluctuation in the nitride film thickness rather not due to any chemical inhomogeneity.

#### 4. Discussion

From our STM studies of silicon nitride formation it is quite clearly that the initial  $\text{Si}_3\text{N}_4$  nucleation always starts at the surface steps of Si(111) substrate in two ways: (a) in one hand direct formation of nucleation patches at the step edges of initial Si(111) surface or (b) on other hand formation of additional steps by creating triangular nucleation etch pits within the  $7 \times 7$ -Si(111) terrace areas. Initial nucleation at the surface steps can be correlated to the defect induced nucleation of N atom. As more dangling bonds are available at the step edges, they act as chemically more active with respect to the terrace area of  $7 \times 7$ -Si(111) domains. As a result, it can facilitate the initial nucleation of nitride layer. In addition, surface steps give more degrees of freedom for the nitride layer growth leading towards the relaxation of nitride lattice strain induced from the mismatch between the deposited nitride material and the Si substrate lattice.

Larger size of the nitride nucleation centers with a lower number density for higher nitridation temperature are explained in terms of enhanced thermal diffusion of the N and Si adatoms. Thermal diffusion starts to dominate above 750°C, which results in a heterogeneous nucleation of pits/patches at substrate defects, i.e. at Si(111)- $7 \times 7$  domain boundaries and surface steps.  $\text{Si}_3\text{N}_4$  nucleation above 850°C



occurs exclusively at the surface steps, which can be concluded as follows. There are no such domain boundaries of  $7 \times 7$  structure due to surface phase transition at about  $830^\circ\text{C}$  from the  $(7 \times 7) \rightarrow (1 \times 1)$  [37]. Moreover, at higher nitridation temperature the surface diffusion of Si and N adatoms gets larger. The triangular shape of the etch pits/patches may be influenced by the three-fold crystal symmetry of the underlying Si(111)- $7 \times 7$  substrate.

Morphological changes during post-annealing as well as improvement in structural quality can also be attributed to the temperature induced enhanced surface diffusion of Si and N adatoms. In one hand, high temperature promotes a better diffusion of surface Si atoms. On other hand, crystalline  $\text{Si}_3\text{N}_4$  formation under atomic N exposure demands a proper supply of adatom species. Hence, an improvement in crystalline quality is expected for the higher nitridation temperature. LEED observations can also be explained in a very similar manner. The continuous supply of Si atoms can be linked to groove and hole formation on Si(111) surface by removal of the upper terrace. This will act as a Si source for further nitride formation. The enlargement of nitride nucleation patches or free standing islands can also be explained in terms of coalescence effect or by local nitride re-growth. The transition of free standing nitride islands from a triangular to truncated /distorted-hexagonal shape can be explained by crystal rotational symmetry *i.e.*, three fold symmetry of Si(111) and the hexagonal symmetry of  $\text{Si}_3\text{N}_4$ . Nitride nucleation through etch pits formation around the domain boundary of initial Si(111)- $7 \times 7$  is also related to defect induced nucleation, as found for nitridation along surface steps. 2D islands of  $\text{Si}_3\text{N}_4$  with multiple steps/ step bunching can be explained as follows. Outer diffusion of Si-atoms can easily occur at the step-edges and it can act as a source for Si atoms for further nitride formation. In this way, steps are getting larger and deeper with nitridation temperature and provide the Si supply. As a result, it turns in to a deep crack formation. This type of surface morphology is generally found for 'quadruplet structures' where the growth temperature usually stays above  $1000^\circ\text{C}$ . However, for saturation thickness flat terrace area with little roughening is observed, which might be due to the ion induced damage, caused by the long exposure of plasma source.

The atomically resolved honey-comb like " $8 \times 8$ " surface reconstruction of the  $\beta\text{-Si}_3\text{N}_4$  (0001) surface can only be observed for very thin nitride films (coverage below 2ML), which appears in a loop like way. In addition, no real long range symmetry has been found in STM imaging. This honeycomb-like appearance with many local disordering in STM images can be correlated in following ways. In one hand, the STM images can easily get influenced by the  $\text{Si}_3\text{N}_4$ -Si(111) interface states (very thin film). As there is a significant lattice mismatch between the substrate and epilayer, it may lead to a highly distorted bonding configuration. On other hand, STM imaging can also be modulated by the local electronic states of underlying Si(111) substrate (only valid for thin overlayer). In contrast, " $8/3 \times 8/3$ " super structures show a clear atomic reconstructions with long range symmetry. As it appears for a relatively thicker layer, background electronic influence such as sub-surface information can be ignored. However, a weak three fold surface modulation has been observed for thicker nitride films which is in good agreement with the proposed structural model of Bauer et al. [13]

STM findings of roughening of the silicon nitride surface at higher nitridation temperature are also complementary with our ESCA microscopy results. Nitride films appear as chemically homogeneous, however, contrast in the ESCA images are mostly due to the thickness fluctuation of the nitride film. The stoichiometry, *i.e.*, chemical composition of the nitride films is found to be  $\text{Si}_3\text{N}_4$  for both, smooth and rough surface morphology nitride films grown at lower and higher nitridation temperatures, respectively. The contrast in ESCA microscopy is only observed for higher nitridation temperatures as it results in formation of nitride films of inhomogeneous thickness.

## 5. Conclusions

In summary, high quality crystalline silicon nitride thin films have successfully been grown on clean Si(111) substrate by elevated temperature exposure of active nitrogen from a RF-plasma source. Initial nucleation process, nitridation temperature and atomic N exposure duration dependent films structure and morphology, surface atomic reconstructions and chemical properties of the  $\beta$ -Si<sub>3</sub>N<sub>4</sub>/Si(111) have been investigated in details using different surface characterization techniques such as STM, LEED and ESCA microscopy. Initial Si<sub>3</sub>N<sub>4</sub> nucleation strongly determine by the Si(111) surface defects. It always occurs at the step edges (upper terrace) and terraces by nucleation pit formation. Lower nitridation temperature generally results in nitride films of poor crystalline quality but appears with a smooth surface morphology. Whereas, a highly crystalline Si<sub>3</sub>N<sub>4</sub> film can be achieved for nitridation at higher temperatures. Moreover, the surface morphology gets severely roughen by forming holes and grooves on Si(111) terrace. An atomically resolved honeycomb-like reconstruction of “8 × 8” surface periodicity is observed for very thin Si<sub>3</sub>N<sub>4</sub> films. However, for thicker films grown at higher nitridation temperature shows an atomically resolved “8/3 × 8/3” superstructure in STM. Both the findings are complementary and in good agreement with LEED results. ESCA microscopy measurements confirm a Si<sub>3</sub>N<sub>4</sub> stoichiometry of the nitride films. It also suggests a thickness fluctuation for a nitride growth at higher temperature. Finally, this type of crystalline Si<sub>3</sub>N<sub>4</sub> films have a huge potential to successfully replace the existing SiO<sub>2</sub> dielectric layer on Si(111) for device technology. Furthermore, it can also provide a platform for crystalline growth of group III nitrides on Si(111), which can further integrate the optoelectronic devices to the existing well established Si based technology [38].

## Acknowledgements


The author is very much grateful to Prof Jens Falta and his coworkers of University of Bremen, Germany, for all kind of experimental supports as well as all short of valuable scientific knowledge and discussions.

## Author details

Subhashis Gangopadhyay  
Department of Physics, Birla Institute of Technology and Science (BITS) Pilani,  
Rajasthan, India

\*Address all correspondence to: [subha@pilani.bits-pilani.ac.in](mailto:subha@pilani.bits-pilani.ac.in)

## IntechOpen

© 2020 The Author(s). Licensee IntechOpen. Distributed under the terms of the Creative Commons Attribution - NonCommercial 4.0 License (<https://creativecommons.org/licenses/by-nc/4.0/>), which permits use, distribution and reproduction for non-commercial purposes, provided the original is properly cited. 

## References

- [1] Watanabe M, Suemasu T, Murakami S, Asada M. Negative differential resistance of metal ( $\text{CoSi}_2$ )/insulator ( $\text{CaF}_2$ ) triple-barrier resonant tunneling diode. *Applied Physics Letters*. 1993;**62**:300
- [2] Jiang X, van Dijken S, Parkin SSP. Giant magnetocurrent exceeding 3400% in magnetic tunnel transistors with spin-valve base layers. *Applied Physics Letters*. 2002;**80**:3364
- [3] Garfunkel E, Gusev EP, Vul A, editors. *Fundamental Aspects of Ultrathin Dielectrics on Si-Based Devices*. Dordrecht: Kluwer Academic Publishers; 1998
- [4] Gusev EP, Lu H-C, Garfunkel EL, Gustafsson T, Green ML. Growth and characterization of ultrathin nitrided silicon oxide films. *IBM Journal of Research and Development*. 1999;**43**:265
- [5] Tsai S-J, Wang C-L, Lee H-C, Lin C-Y, Chen J-W, Shiu H-W, et al. Approaching defect-free amorphous silicon nitride by plasma-assisted atomic beam deposition for high performance gate dielectric. *Scientific Reports*. 2016;**6**:28326
- [6] Gangopadhyay S, Schmidt T, Falta J. N-plasma assisted MBE grown GaN films on Si(111). *Physica Status Solidi B*. 2006;**243**:1416
- [7] Nakada Y, Aksenov I, Okumura H. GaN heteroepitaxial growth on silicon nitride buffer layers formed on Si (111) surfaces by plasma-assisted molecular beam epitaxy. *Applied Physics Letters*. 1998;**73**:827
- [8] Liu AY, Cohen ML. Structural properties and electronic structure of low-compressibility materials:  $\beta\text{-Si}_3\text{N}_4$  and hypothetical  $\beta\text{-C}_3\text{N}_4$ . *Physical Review B*. 1990;**41**:10727
- [9] Gruen R. The crystal structure of  $\beta\text{-Si}_3\text{N}_4$ : Structural and stability considerations between  $\alpha$ - and  $\beta\text{-Si}_3\text{N}_4$ . *Acta Crystallographica. Section B*. 1979;**35**:800
- [10] Hitchman MA, Jensen KF. *Chemical vapour deposition*. London: Academic Press; 1993
- [11] van Bommel AJ, Meyer E. A low energy electron diffraction study of the  $\text{PH}_3$  adsorption on the Si (111) surface. *Surface Science*. 1967;**8**:381
- [12] Kubler L, Bischo JL, Bolmont D. General comparison of the surface processes involved in nitridation of Si(100)- $2\times 1$  by  $\text{NH}_3$  and in  $\text{SiN}_x$  film deposition: A photoemission study. *Physical Review B*. 1988:13113
- [13] Bauer E, Wei Y, Mueller T, Pavlovskaya A, Tsong IST. Reactive crystal growth in two dimensions: Silicon nitride on Si(111). *Physical Review B*. 1995;**51**:17891
- [14] Yoshimura M, Takahashi E, Yao T. Initial stages of the nitridation of the Si(111) surface observed by scanning tunneling microscopy. *Journal of Vacuum Science and Technology B*. 1996;**14**:1048
- [15] Wang X-S, Zhai G, Yang J, Cue N. Crystalline  $\text{Si}_3\text{N}_4$  thin films on Si(111) and the  $4\times 4$  reconstruction on  $\text{Si}_3\text{N}_4(0001)$ . *Physical Review B*. 1999;**60**:R2146
- [16] Zhai G, Yang J, Cue N, Wang X-S. Surface structures of silicon nitride thin films on Si(111). *Thin Solid Films*. 2000;**366**:121
- [17] Ahn H, Wu C-L, Gwo S, Wei CM, Chou YC. Structure determination of the  $\text{Si}_3\text{N}_4/\text{Si}(111)-(8\times 8)$  surface: A combined study of Kikuchi electron holography, scanning



tunneling microscopy, and ab initio calculations. *Physical Review Letters*. 2001;**86**:2818

[18] Wiggins MD, Baird RJ, Wynblatt P. Thermal nitridation of Si(111) by nitric oxide. *Journal of Vacuum Science and Technology*. 1981;**18**:965

[19] Nishijima M et al. Reactions of NO with the Si(111) (7 × 7) surface: EELS, LEED and AES studies. *Surface Science*. 1984;**137**:473

[20] Avouris P, Wolkow R. Atom-resolved surface chemistry studied by scanning tunneling microscopy and spectroscopy. *Physical Review B*. 1989;**39**:5091

[21] Roettger B, Kliese R, Neddermeyer H. Adsorption and reaction of NO on Si(111) studied by scanning tunneling microscopy. *Journal of Vacuum Science and Technology B*. 1996;**14**:1051

[22] Ha JS, Park K-H, Yun WS, Lee E-H, Park S-J. Evolution of surface morphology in the initial stage of nitridation of the Si(111)-7×7 surface by nitrogen ions. *Journal of Vacuum Science and Technology B*. 1997;**15**:1893

[23] Ha JS, Park K-H, Yun WS, Lee E-H, Park S-J. Interaction of low-energy nitrogen ions with an Si(111)-7×7 surface: STM and LEED investigations. *Applied Physics A: Materials Science & Processing*. 1998;**66**:S495

[24] Ha JS, Park K-H, Yun WS, Lee E-H. Nanometer scale selective etching of Si(111) surface using silicon nitride islands. *Journal of Vacuum Science and Technology B*. 1998;**16**:2806

[25] Ha JS, Park K-H, Yun WS, Ko Y-J, Kim SK. Interaction of nitrogen with Si(111)-7×7 surfaces at elevated temperatures. *Surface Science*. 1999;**426**:373

[26] Morita Y, Tokumoto H. Origin of the 8/3×8/3 superstructure in STM images of the Si(111)-8×8:N surface. *Surface Science*. 1999;**443**:L1037

[27] Morita Y, Tokumoto H. Bias-dependent atomic images of a quadruplet silicon-nitride monolayer on the Si(111) surface. *Surface Science*. 2000;**466**:L802

[28] Yamabe N, Yamamoto Y, Ohachi T. Epitaxial growth of b-Si<sub>3</sub>N<sub>4</sub> by the nitridation of Si with adsorbed N atoms for interface reaction epitaxy of double buffer AlN(0001)/b-Si<sub>3</sub>N<sub>4</sub>/Si(111). *Physica Status Solidi C: Current Topics in Solid State Physics*. 2011;**8**:1552

[29] Mansurov VG, Malina TV, Galitsyn YG, Shklyayev AA, Zhuravlev KS. Kinetics and thermodynamics of Si(111) surface nitridation in ammonia. *Journal of Crystal Growth*. 2016;**441**:12

[30] Wu C-L, Chen W-S, Su Y-H. N<sub>2</sub>-plasma nitridation on Si(111): Its effect on crystalline silicon nitride growth. N<sub>2</sub>-plasma nitridation on Si(111): Its effect on crystalline silicon nitride growth. *Surface Science*. 2012;**606**:L51

[31] Tabe M, Yamamoto T. Initial stages of nitridation of Si(111) surfaces: X-ray photoelectron spectroscopy and scanning tunneling microscopy studies. *Surface Science*. 1997;**376**:99

[32] Gangopadhyay S, Schmidt T, Falta J. Initial stage of silicon nitride nucleation on Si(111) by rf plasma-assisted growth. *Surface Science and Nanotechnology*. 2006;**4**:84

[33] Ermolieff A, Bernard P, Marthon S, Camargo da Costa J. Nitridation of Si (100) made by radio frequency plasma as studied by in situ angular resolved x-ray photoelectron spectroscopy. *Journal of Applied Physics*. 1986;**60**:3162

[34] Aballe L, Gregoratti L, Barinov A, Kiskinova M, Clausen T, Gangopadhyay S, et al. Interfacial interactions at Au/Si<sub>3</sub>N<sub>4</sub>/Si(111) and Ni/Si<sub>3</sub>N<sub>4</sub>/Si(111) structures with ultrathin nitride films. *Applied Physics Letters*. 2004;**84**:5031

[35] Schmidt T, Clausen T, Gangopadhyay S, Falta J, Heun S, Gregoratti L, et al. Spectro-microscopy of ultra-thin SiN films on Si (111). *Nuclear Instruments and Methods in Physics Research Section B*. 2003;**200**:79

[36] Falta J, Schmidt T, Gangopadhyay S, Clausen T, Brunke O, Flege JI, et al. Ultra-thin high-quality silicon nitride films on Si(111). *Europhysics Letters*. 2011;**94**:16003

[37] Fukaya Y, Shigeta Y. New phase and surface melting of Si(111) at high temperature above the (7×7)–(1×1) phase transition. *Physical Review Letters*. 2000;**85**:5150 and references therein

[38] Chen W-C, Yu T-Y, Lai F-I, Chen H-P, Lin Y-W, Kuo S-Y. Growth of catalyst-free hexagonal pyramid-like InN nanocolumns on nitrated Si(111) substrates via radio-frequency metal–organic molecular beam epitaxy. *Crystals*. 2019;**9**:291